

Surface Science Letters

# Photon mapping of MgO thin films with an STM

H.M. Benia, N. Nilius<sup>\*</sup>, H.-J. Freund

*Fritz-Haber-Institut der Max-Planck-Gesellschaft, Faradayweg 4-6, D-14195 Berlin, Germany*

Received 21 December 2006; accepted for publication 8 March 2007

Available online 18 March 2007

## Abstract

The light emission from an STM junction consisting of an MgO thin film on Mo(001) and an Au tip is analyzed with respect to its spatial distribution for various excitation conditions. The spectral characteristic of the light is compatible with an emission mechanism mediated by tip-induced plasmons that are excited by inelastic electron tunneling involving field-emission resonances in the tip–sample gap. The dependence of field-emission resonances on the MgO work function allows the controlled stimulation of differently thick oxide islands in the photon maps by changing the sample bias.

© 2007 Elsevier B.V. All rights reserved.

*Keywords:* STM; Oxide films; Optical properties; Work function

Wide band-gap insulators, such as simple oxides or alkali-halogenides, exhibit a rich optical behavior, characterized by various excitation and deexcitation channels with sub band-gap energy [1–4]. The diversity of optical modes is related to structural imperfections in the crystal lattice, such as point defects, step or corner atoms. Responsible for their smaller activation energies compared to bulk modes is the reduced Madelung potential at lattice sites with lower coordination [5,6]. The energy of local optical modes therefore decreases when going from high-coordinated bulk sites towards surface, step and corner sites of the insulator. The interplay between structural and local optical properties is mediated by mobile electron–hole pairs (excitons), which are able to transport excitation energy from the preferred absorption to the emission centers of the crystal in a diffusive motion.

Thus far, connection between structural and optical properties of wide band-gap insulators has only been established in an indirect manner [2,3,7]. The approach is based on the preparation of nano-crystallites exposing an abundance of one specific surface site, whose optical fingerprint is then detected with a non-local spectroscopic technique.

Direct correlation would require an optical method that provides spatial resolution on the length scale of the distance between neighboring optical centers, e.g. between two corner or kink sites. Optical analysis with nanometer spatial resolution can, in principle, be achieved by scanning near field optical microscopy and photon emission spectroscopy performed with a scanning tunneling microscope (STM).

The latter method, which has been established by Berndt and Gimzewski, exploits the efficient excitation of optical modes in the tip–sample gap of an STM by electron/hole injection from the tip [8]. The technique was successfully employed to investigate the local optical properties of noble metal and semiconductor surfaces, quantum dots, metal particles and single molecules [8–12]. In this letter, we report on the photon emission from MgO thin films stimulated by electron injection from an Au tip. MgO is a prototype material for a wide band-gap insulator and should therefore exhibit optical activity originating from the radiative decay of excitons at low-coordinated surface sites [13]. However, strong electromagnetic interactions between tip and sample are identified as the main channel for the observed light emission from the tunnel junction.

The experiments are performed with an UHV–STM operated at liquid nitrogen temperature [14]. The Beetle-type

<sup>\*</sup> Corresponding author. Tel.: +49 30 84134191; fax: +49 30 84134101.  
E-mail address: [nilius@fhi-berlin.mpg.de](mailto:nilius@fhi-berlin.mpg.de) (N. Nilius).

microscope head is surrounded by a parabolic mirror, which collects photons from the tunnel junction and reflects them out of the vacuum chamber. After passing a quartz view port, the light is either guided to a spectrograph coupled to a CCD detector for spectral analysis or to a photo-multiplier tube for fast and sensitive detection. The latter option is employed to produce ‘photon maps’ of the sample surface, where an STM topographic image is recorded simultaneously with a map of the local emission yield, generated by the photo-multiplier output. The MgO thin films are prepared by Mg deposition onto a clean Mo(001) surface in  $10^{-7}$  mbar oxygen atmosphere. Subsequent annealing to 1000 K stimulates crystallization of the MgO layer into a pseudomorphic lattice, where the Mo[110] direction aligns with the MgO[100]. In the investigated thickness regime, the film is partially relaxed towards the intrinsic MgO lattice constant via introduction of a dislocation network and mosaic formation. The complete structural evolution of the MgO/Mo(001) system with film thickness is summarized in an earlier paper [13]. Electrochemically etched Au and PtIr wires are used as tip material.

A characteristic STM image of a 7 ML thick MgO film grown on Mo(001) is shown in Fig. 1A. The surface morphology is dominated by large oxide islands separated by non-polar [100] oriented trenches of 4–8 Å depth. Such trenches open up to release stress and strain in the oxide surface that originates from the 5% lattice mismatch with the Mo support. Photon maps of the oxide film taken with an Au tip are presented in Fig. 2 as a function of sample bias. Intensive light emission is detected in the bias range between 4.0 and 7.0 V. In the low-bias regime, the emission is spatially confined to the center of large oxide terraces. The optically active areas increase in size with sample bias until the whole top-most MgO layer appears bright at around 5.0 V. Further voltage increase causes a fast decline of the photon response from upper oxide terraces, while lower-lying MgO areas become bright. The second-highest MgO layer emits light at around 6.0 V, while only deep

holes in the oxide participate in the emission process at even higher bias. Apparently, the oxide layer showing optical activity can be selected via the sample bias, whereby lower voltages are required to stimulate thicker oxide patches.<sup>1</sup>

The spectral distribution of the emitted light is analyzed as a function of sample bias and surface location using the CCD detector (Fig. 1B). The intensity is peaked at 750–800 nm ( $\sim 1.6$  eV), and shows rather small dependence on excitation conditions and tip position during spectroscopy. High emission yields are exclusively obtained for carefully prepared Au tips, while PtIr tips produce almost no photon signal from the MgO surface.

From the spectral characteristics and the excitation behavior, the mechanism of light emission from the tunnel junction can be deduced. An emission peak at approximately 1.6 eV is not compatible with intrinsic emission properties of MgO, where features at significantly higher energies are expected. Relevant optical channels in MgO, such as exciton decays at corner and step sites, produce photons of 3.0–4.5 eV energy [1–3]. Also the dependence of the emission characteristic from sample bias and tip material (Au versus PtIr) is in conflict with an emission process controlled by intrinsic MgO exciton modes. The widely accepted explanation for light emission from a tunnel contact formed by two metal electrodes involves stimulation and radiative decay of tip-induced plasmons (TIP's) that are excited by inelastically tunneling electrons [8,15,16]. The model successfully predicts the spectral characteristics of the emitted light on the basis of the dielectric functions of tip and sample. It also rationalizes the role of the bias voltage, as the parameter that controls the tip-sample distance and therewith the excitation cross-section for TIP modes. In the present experiment, the Au tip and the Mo surface play the active parts in supporting the TIP's, while the MgO layer primarily acts as dielectric spacer in addition to the vacuum gap between tip and sample. The tip dominates the spectral characteristics of the emitted light, because the small imaginary part of the Au dielectric function reduces the effect of plasmon damping in the tip electrode [16]. The interpretation is in agreement with earlier experiments on tunnel contacts containing an Au electrode, where emission peaks at around 800 nm were frequently observed [15,17,18]. An emission mechanism involving TIP's is additionally supported by the fact that replacing the Au tip by PtIr weakens the photon signal, as expected from the high dielectric losses of PtIr in the visible range.

Even though the MgO plays a more passive role in a plasmon-mediated emission process due to its negligible free-electron density, a certain contribution is concluded from the different photon yields detected for MgO islands of different height. The role of the MgO layer in the emis-

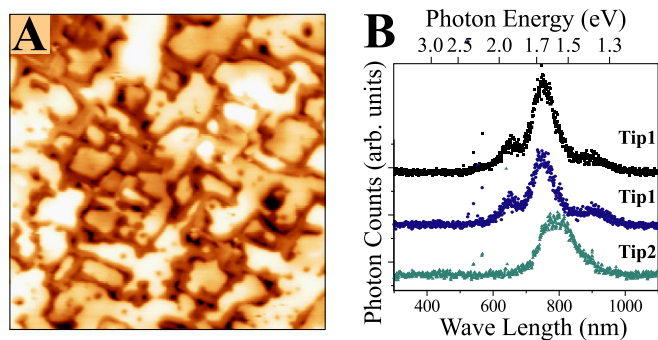


Fig. 1. (A) STM topographic image of 7 ML MgO grown on Mo(001) ( $125 \times 125 \text{ nm}^2$ ). A sample bias of 5 V and a current of 40 pA were chosen for imaging. (B) Photon emission spectra from the tunnel junction measured with 5.0 V sample bias and 2 nA current. The upper two spectra were taken with the same Au tip at different surface locations, while the lower one was obtained with a differently prepared Au tip.

<sup>1</sup> Absolute calibration of the MgO layer thickness is not possible from the STM topographic images and high/low oxide patches refer only to the nominal film thickness of 7 ML.

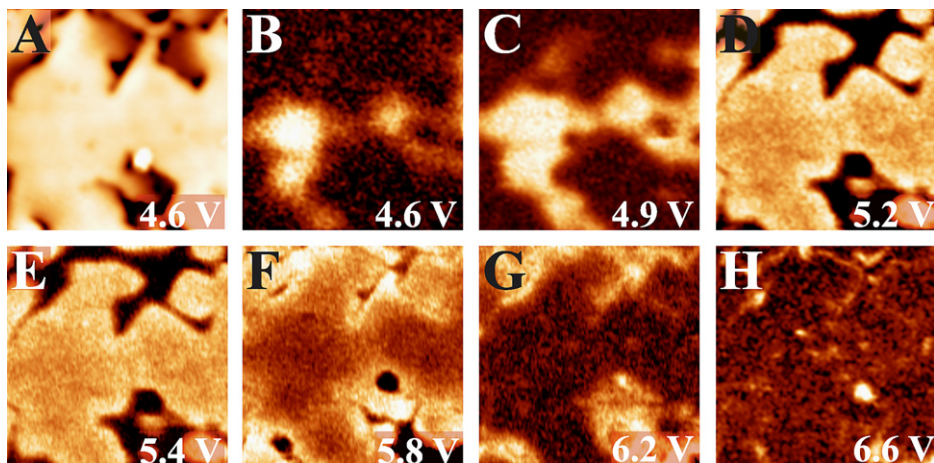


Fig. 2. (A) Topographic image and (B–H) corresponding photon maps of MgO/Mo(001) ( $40 \times 40 \text{ nm}^2$ ) taken at 2 nA electron current and the given sample voltages. The photon signal was detected with a photo-multiplier tube.

sion process is twofold. (i) It increases the dielectric constant in a substantial part of the gap by almost one order of magnitude ( $\epsilon_{\text{MgO}} = 10$ ). The dielectric step occurring at the MgO surface refracts the field lines of electromagnetic gap modes towards the tip–sample axis, which leads to a concentration of the plasmon field under the tip and increases the radiated power. (ii) Due to its insulating character, the oxide layer is able to channel electrons into elastic or inelastic tunnel paths depending on the applied bias. It therefore affects the cross-section for TIP-mediated emission processes, as sketched in the following.

For relatively thick insulating films, sufficient electron transport is realized only at high sample voltages ( $V_{\text{sample}} > 4.0 \text{ V}$ ), where electrons leave the tunnel barrier and propagate as free carriers between tip and sample (field emission mode) [19,20]. The differential conductance in this regime is governed by field-emission resonances (FER's), which can be viewed as standing electron waves occurring when free-electron wave functions match the geometry of the classically accessible part of the tip–sample gap. Such resonances are characterized by an extremely high electron transmission probability and carry a large portion of the current at elevated voltages. The bias position of FER's can be determined from distance–voltage spectra ( $dz/dV$ ) taken with enabled feedback loop, because steep rises in the conductance induce sudden changes in the tip–sample separation ( $z$ ) and show up as pronounced maxima in  $dz/dV$  spectra. The  $dz/dV$  curves in Fig. 3A, measured on differently high MgO islands, clearly reveal the oscillatory behavior expected when passing through a series of FER's. Apparently, the spectra of the two MgO islands are shifted against each other by 0.65 eV, which relates to the dependence of resonance energies on the sample work function [21] and indicates variation of this quantity with MgO film thickness. Indeed, the work function of thin oxide films was found to depend on the layer thickness, and decreases for the MgO/Mo system from 4.5 eV for pure Mo(001) to below 3.0 eV for a 3 ML thick MgO film [22,23]. The

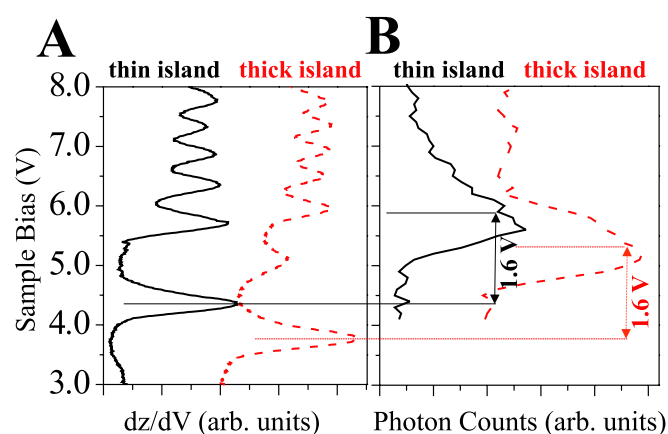


Fig. 3. (A) Variation of tip-height with sample bias ( $dz/dV$  spectrum) measured for a thin (left) and a thick (right) MgO island. An electron current of 20 pA was stabilized during spectral acquisition by the feedback loop. The height signal was numerically differentiated. Maxima in the  $dz/dV$  spectra correspond to the field-emission resonances. (B) Photon-intensity versus bias plot acquired with a photo-multiplier tube for a constant electron current of 1.0 nA. The maximum occurs at the position of the first FER plus the energy to excite a TIP in the tunnel gap, indicative for an emission mechanism determined by inelastic electron tunneling through the first FER.

work-function change can be attributed to (i) the compression of the intrinsic dipole layer at the metal–oxide interface and (ii) the reduction of image potential interactions due to the dielectric film in front of the Mo surface. As a result of the work-function decrease, thick MgO islands feature field-emission resonances at lower bias compared to thinner patches or bare Mo(001) [23]. From the maximum shift of the first FER, a work-function drop of approximately 1.5 eV is estimated between clean Mo(001) and a 7 ML thick oxide film, in agreement with theoretical considerations [22].

In analogy to the elastic tip–sample current, also the inelastic tunneling probability and therefore the excitation cross-section for TIP's is affected by the field-emission

resonances [24,25]. High photon yields are expected whenever the final state of an inelastic tunneling process matches a FER of high electron transmissibility. In this case, the elastic to inelastic tunneling ratio significantly shifts towards the inelastic contribution, an effect that is amplified by the generally low electron conductance through the insulating oxide film. The photon-intensity versus voltage plot in Fig. 3B provides an experimental verification for this relation. High emission yield is detected for a sample bias that corresponds to the position of the first FER plus the energy to excite a TIP in the tunnel contact. The maxima in elastic electron transport and in photon yield are separated by 1.6 eV, which agrees well with the energy of the plasmon mode. Whereas several FER's are detectable in the elastic tunnel path, only the first resonance enhancement emerges in the light emission channel. This behavior is the consequence of a sharply decreasing plasmon excitation probability for increasing tip-sample distance [8].

An alternative emission mechanism based on the radiative transition of electrons between two FER's cannot be ruled out here [26]. Although the energy separation between the first two FER levels (1.3 eV) is smaller than the detected photon energy, this is not necessarily an exclusion criterion, as FER's sensitively depend on tip shape and tunnel current. Discrimination between the two proposed mechanisms becomes feasible for tip materials, where the energy of the TIP mode is clearly larger than the typical separation between two FER's. Corresponding experiments using Ag tips are currently in progress.

Summarizing the arguments discussed so far, the stimulation of differently high MgO layers in STM photon maps can be traced back to an interplay between a modulated inelastic tunneling probability mediated by FER's and their dependence on the oxide film thickness via the work function. At low sample bias, optical modes are excited above the center of high MgO islands, where the work function is small and the FER levels are lowest in energy. At around 5.0 V, the emission mechanism becomes efficient for the whole top-most MgO layer, which brightly contrasts against lower MgO terraces in the photon maps. Further bias increment shifts the resonance condition gradually towards thinner oxide patches, which are characterized by high-lying FER levels. These topographically lower sample areas appear bright in photon maps taken above 6.0 V sample bias.

In conclusion, spatially resolved light emission has been detected from an MgO thin film grown on Mo(001) by means of photon mapping with an STM. Although the emission mechanism is governed by the radiative decay of tip-induced plasmons excited in the Au–Mo junction, the presence of the MgO dielectric film strongly modifies the emission characteristics of the tunnel gap. Exploiting the decreasing MgO work function with increasing layer thickness enables a tuning of optical activity towards oxide

islands of different height. Intrinsic optical excitations of the MgO film are not accessible to this experiment due to the significant energy gap between the oxide excitons ( $E_{\text{exc}} > 3.0$  eV) and collective TIP modes in the tunnel gap ( $E_{\text{TIP}} \sim 1.6$  eV). A different choice of the tip material to shift the TIP towards intrinsic MgO excitations might enable the spatially resolved analysis of optical properties of thin MgO films in the future.

## References

- [1] M. Anpo, Y. Yamada, Y. Kubokawa, S. Coluccia, A. Zecchina, M. Che, *J. Chem. Soc., Faraday Trans.* 1 84 (1988) 751.
- [2] S. Stankic, M. Muller, O. Diwald, M. Sterrer, E. Knözinger, J. Bernardi, *Angew. Chem. Int. Ed.* 44 (2005) 4917; S. Stankic, J. Bernardi, O. Diwald, E. Knözinger, *J. Phys. Chem. B* 110 (2006) 13866.
- [3] R. Hacquart, J.M. Krafft, G. Costentin, J. Jupille, *Surf. Sci.* 595 (2005) 172.
- [4] W.P. Hess, A.G. Joly, K.M. Beck, M. Henyk, P.V. Sushko, P.E. Trevisanutto, A.L. Shluger, *J. Phys. Chem. B* 109 (2005) 19563.
- [5] A. Stashans, E. Kotomin, J.L. Calais, *Phys. Rev. B* 49 (1994) 14854.
- [6] A.L. Shluger, P.V. Sushko, L.N. Kantorovich, *Phys. Rev. B* 59 (1999) 2417; P.V. Sushko, J.L. Gavartin, A.L. Shluger, *J. Phys. Chem. B* 106 (2002) 2269.
- [7] J. Kramer, C. Tegenkamp, H. Pfnür, *Phys. Rev. B* 67 (2003) 235401.
- [8] R. Berndt, in: R. Wiesendanger (Ed.), *Scanning Probe Microscopy*, Springer Series Nanoscience and Technology, Springer, Berlin, 1998, p. 97.
- [9] C. Thirstrup, M. Sakurai, K. Stokbro, M. Aono, *Phys. Rev. Lett.* 82 (1999) 1241.
- [10] U. Hakanson, M.K. Johansson, M. Holm, C. Pryor, L. Samuelson, W. Seifert, *Appl. Phys. Lett.* 81 (2002) 4443.
- [11] N. Nilius, N. Ernst, H.-J. Freund, *Phys. Rev. Lett.* 84 (2000) 3994.
- [12] X.H. Qui, G.V. Nazin, W. Ho, *Science* 299 (2003) 542.
- [13] S. Benedetti, H.M. Benia, N. Nilius, H.-J. Freund, *Chem. Phys. Lett.* 430 (2006) 330.
- [14] N. Nilius, A. Cörper, G. Bozdech, N. Ernst, H.-J. Freund, *Prog. Surf. Sci.* 67 (2001) 99.
- [15] R. Berndt, J.K. Gimzewski, P. Johansson, *Phys. Rev. Lett.* 67 (1991) 3796.
- [16] P. Johansson, R. Monreal, P. Apell, *Phys. Rev. B* 42 (1990) 9210.
- [17] K. Ito, S. Ohyama, Y. Uehara, S. Ushioda, *Surf. Sci.* 324 (1995) 282.
- [18] M.M. Bischoff, M.C. van der Wielen, H. van Kempen, *Surf. Sci.* 400 (1998) 127.
- [19] G. Binnig, K.H. Frank, H. Fuchs, N. Garcia, B. Reihl, H. Rohrer, F. Salvan, A.R. Williams, *Phys. Rev. Lett.* 55 (1985) 991.
- [20] E.D.L. Rienks, N. Nilius, H.-P. Rust, H.-J. Freund, *Phys. Rev. B* 71 (2005) 241404.
- [21] O.Y. Kolesnychenko, Y.A. Kolesnichenko, O.I. Shklyarevskii, H. van Kempen, *Physica B* 291 (2000) 246.
- [22] L. Giordano, F. Cinquini, G. Pacchioni, *Phys. Rev. B* 73 (2005) 045414.
- [23] S. Schintke, S. Messerli, M. Pivetta, F. Patthey, L. Libjoulle, M. Stengel, A. de Vita, W.D. Schneider, *Phys. Rev. Lett.* 87 (2001) 276801.
- [24] R. Berndt, J.K. Gimzewski, *Ann. Phys.* 2 (1993) 133.
- [25] F. Silly, O. Gusev, E. LeGoff, L. Barbier, F. Charra, *EuroPhys. Lett.* 64 (2003) 475.
- [26] G. Hoffmann, J. Kliewer, R. Berndt, *Phys. Rev. Lett.* 87 (2001) 176803.